Al-Rafidain J Med Sci. 2026;10(1):254-264.
DOI: https://doi.org/10.54133/ajms.v10i1.2693

AJMS

Online ISSN (3219-2789)

Research Article

Griseofulvin Nanosuspension: A Quality by Design Approach to Enhance the Dissolution Performance

Sarah Salim Oleiwi*, Ghaidaa Sulaiman Hameed
Department of Pharmaceutics, College of Pharmacy, Mustansiriyah University, Baghdad, Iraq
Received: 25 December 2025; Revised: 22 February 2026; Accepted: 3 March 2026

Abstract

Background: Griseofulvin (GF) is a BCS class II antifungal drug characterized by poor aqueous solubility with low and variable oral bioavailability, which affects its therapeutic performance. ***Objective***: This study aimed to optimize a stable griseofulvin nanosuspension (NS) using an ultrasonication-assisted antisolvent precipitation method combined with a Quality by Design (QbD) approach. ***Methods***: Preliminary stabilizer screening identified polyvinylpyrrolidone K30 (PVP) and sodium lauryl sulfate (SLS) as the most effective electrosteric stabilizer system. Box–Behnken design was used to study the effects of surfactant and polymer percent, in addition to sonication time, on particle size (PS) and polydispersity index (PDI). The optimized nanosuspension was lyophilized using trehalose or mannitol. as cryoprotectants. Physicochemical characterization was performed using particle size analysis, zeta potential, PXRD, DSC, and FTIR, while solubility, dissolution, and stability studies were also conducted. ***Results***: The optimized formulation exhibited 264±32.7 nm as PS, a PDI of 0.246±0.02, an entrapment efficiency of 91±3.44%, and a zeta potential of −28.7 mV, indicating good colloidal stability. Trehalose provided superior redispersibility and demonstrated significantly enhanced solubility and rapid dissolution, achieving 96% drug release within 15 min, compared with mannitol. Solid-state characterization confirmed a marked reduction in crystallinity and partial amorphization of GF. Stability studies confirmed acceptable physicochemical stability under accelerated storage conditions. ***Conclusions***: Overall, the developed griseofulvin nanosuspension represents a promising strategy for improving the solubility and dissolution behavior of poorly water-soluble drugs.

Keywords: Box–Behnken design; Cryoprotectant; Lyophilization; Nanosuspension; Particle size; Stability.

غريزوفلفين كمعلق نانوي: نهج عالي الجودة حسب التصميم لتعزيز قابلية الذوبان

الخلاصة

الخلفية: يُعد الجريسيوفولفين دواءً مضادًا للفطريات من الفئة الثانية حسب التصنيف الحيوي الدوائي، ويتصف بضعف ذوبانيته في الماء وانخفاض توافره الحيوي الفموي، مما ينعكس سلبًا على فعاليته العلاجية. **الهدف**: تطوير نانومعلق مستقر من الجريسيوفولفين باستخدام طريقة الترسيب بالمذيب المضاد المُعزَّزة بالأمواج فوق الصوتية ضمن إطار منهجية مبنية على مبادئ الجودة في التصميم. **الطرائق**: أظهر الفحص الأولي للمثبتات أن مزيج بولي فينيل بيروليدون مع كبريتات لوريل الصوديوم يُعد نظام تثبيت كهروستيريكي فعال. تم استخدام تصميم إحصائي من نوع بوكس–بينكن لدراسة تأثير نسبة المواد الخافضة للتوتر السطحي ونسبة البوليمر وزمن التعريض للأمواج فوق الصوتية على حجم الجسيمات ومعامل تشتتها. تم تجفيف النانومعلق بالتجميد باستخدام التريهالوز أو المانيتول. وقد شملت تقنيات التوصيف تحليل حجم الجسيمات، وقياس جهد الزيتا، وحيود الأشعة السينية، والتحليل الحراري التفاضلي، وقياس أطياف الأشعة تحت الحمراء، بالإضافة إلى دراسة الذوبانية والذوبان والثبات. **النتائج**: أظهر التركيب الدوائي المحسَّن حجم جسيمات بلغ حوالي 264 نانومتر مع تجانس مقبول في التوزيع، وكفاءة احتواء عالية، كما بلغ جهد الزيتا قيمة سالبة تشير إلى ثبات غرواني جيد. وقد تبيّن أن التريهالوز يمنح النانومعلق المجفف قدرة أفضل على إعادة التشتيت بعد الخزن، إضافةً إلى زيادة كبيرة في الذوبانية وسرعة الذوبان، حيث تم الوصول إلى ما يقارب 96% من الجرعة المطلقة خلال 15 دقيقة مقارنةً بالمانيتول. أثبتت دراسات الحالة الصلبة انخفاض درجة التبلور وحدوث تحوّل جزئي نحو الحالة غير المتبلورة مع احتفاظ المستحضر بخصائصه الفيزيائية والكيميائية تحت ظروف الخزن المسرَّع. **الاستنتاجات**: النانومعلق المطوّر للجريسيوفولفين يمثل أسلوبًا واعدًا وفعالًا لتحسين ذوبانية وسرعة ذوبان الأدوية ضعيفة الذوبانية في الماء، مما قد يسهم في تعزيز فعاليتها العلاجية.

* ***Corresponding author***: Sarah S. Oleiwi. Department of Pharmaceutics, College of Pharmacy, Mustansiriyah University, Baghdad, Iraq; Email: saraalobaidy91@uomustansiriyah.edu.iq
Article citation: Oleiwi SS, Hameed GS. Griseofulvin Nanosuspension: A Quality by Design Approach to Enhance the Dissolution Performance. *Al-Rafidain J Med Sci*. 2026;10(1):254-264. doi: https://doi.org/10.54133/ajms.v10i1.2693

INTRODUCTION

Advances in modern drug discovery techniques, such as combinatorial chemistry, computational modeling, and AI-driven screening, have led to the rapid identification of numerous promising drug candidates [1]. However, many of these new molecules possess unfavorable physicochemical properties, including high lipophilicity, large molecular weight, and strong crystal lattices, which result in poor aqueous solubility and variable bioavailability. According to the Biopharmaceutics Classification System (BCS), such compounds are primarily categorized as Class II and IV drugs [2]. To enhance solubility and bioavailability, several formulation approaches have been explored, including salt formation, solid dispersions, cocrystallization, inclusion complexation, and nanotechnology [3]. Nanosuspension is one of the most promising

nanotechnology-based drug delivery systems, particularly for drug candidates that exhibit challenging physicochemical properties. These properties include poor aqueous solubility, the need for relatively high doses, limited salt-forming ability, high molecular weight, elevated lipophilicity (log P), or a high melting point [4]. It is defined as a biphasic colloidal dispersion in which nanosized drug crystals (generally below 1 µm) are dispersed within an aqueous medium. Nanosuspension is physically stabilized through the incorporation of suitable surfactants and/or polymeric stabilizers [5]. This approach has attracted significant interest due to its ability to enhance drug dissolution and oral bioavailability by reducing the particle size into the nanometer range. Such size reduction markedly increases the surface area and the saturation solubility, as explained by the modified Noyes–Whitney relationship and the Gibbs–Thomson effect, ultimately resulting in accelerated dissolution rates [6]. Among the emerging tools for formulation optimization are the Quality by Design (QbD) approach using Response Surface Methodology (RSM) and Box–Behnken Design (BBD). This statistical design enables efficient identification of critical formulation and process variables. In addition, it reduces the number of experiments while systematically studying factor interactions and their effects on responses such as particle size and polydispersity index (PDI) [7]. In this study, griseofulvin (GF), an uncharged, poorly water-soluble antifungal drug, was selected as a model compound to investigate the formulation of nanosuspensions. It is a small molecule with high molecular mobility and a high melting point (217°C-224°C) [8]. It is primarily used for the treatment of fungal infections of the skin, hair, and nails that do not respond to topical treatments, such as ringworm [9]. However, its low aqueous solubility results in incomplete gastrointestinal absorption and low oral bioavailability, posing a significant challenge for formulation scientists and the pharmaceutical industry despite its strong therapeutic potential. Kumar and Siril (2015) employed an evaporation-assisted solvent–antisolvent precipitation technique, using PVP and hydroxypropyl methylcellulose (HPMC) as polymeric stabilizers, and obtained stable nanosuspensions with submicron particle size and enhanced dissolution [10]. Another study on wet-milled griseofulvin nanosuspensions investigated how combining a neutral polymer (hydroxypropyl cellulose, HPC) with an anionic surfactant (sodium dodecyl sulfate, SDS) affects stability. Two molecular weight grades of HPC (SSL and L) were tested at various concentrations, with and without SDS [11]. Sigfridsson *et al*. also formulated griseofulvin nanosuspensions using PVP 1.33% and dioctyl sodium sulfosuccinate (AOT) 0.067% as stabilizers via wet media milling. The optimized nanosuspension achieved higher bioavailability after subcutaneous administration in rats, demonstrating significantly enhanced bioavailability and stability due to synergistic electrosteric stabilization [12].

This study aims to develop and optimize a griseofulvin nanosuspension using an ultrasonication-assisted antisolvent precipitation method and Box–Behnken design to achieve a stable formulation with minimal particle size (PS), low polydispersity index (PDI), and improved dissolution while using a low cryoprotectant percentage during freeze-drying.

METHODS

Materials

Griseofulvin was obtained from Shanghai UCHEM Inc., China, with a purity of >99%. PVP-K30 and Tween 80 were purchased from HiMedia (India). Soluplus® was sourced from BASF (Germany). HPMC-E6 was purchased from Macklin (China). Poloxamer 188 was obtained from Alfa Aesar (USA), SLS from Xi'an Sonwu Biotech (China), and acetone and methanol from Himedia (India), while ethanol was supplied by Honeywell (Germany). Trehalose dihydrate was acquired by Synkote (China), and mannitol was supplied by Alpha Chemika (India). All chemicals and solvents used in this study were of analytical grade.

Stabilizer screening and experiment design

A preliminary screening study was carried out before applying experimental design to select the most suitable stabilizer(s) for achieving the desired particle size (PS). Nanoprecipitation was first performed using individual polymers (HPMC, PVP, poloxamer, and Soluplus®), followed by testing combinations with surfactants such as SLS or Tween 80. All processing parameters were kept constant (solvent: antisolvent ratio 1:10, stirring speed 1000 rpm, and drug concentration 12.5 mg/mL). The polymer–surfactant system that produced the most favorable PS was selected for further optimization. Ultrasonication was then introduced as an additional factor in the Box–Behnken Design to determine whether it provided any further reduction in PS or improvement in PDI beyond the effects of polymer and surfactant concentrations. A three-factor, three-level Box–Behnken Design (BBD) was applied using Design-Expert® Version 13.0.5.0, Stat-Ease Inc., to optimize the nanosuspension formulation variables. Seventeen runs, including four center points, were generated based on three independent factors: SLS percentage (A), polymer percentage within the stabilizer system (B), and sonication time (C), each studied at three coded levels (−1, 0, +1). Particle size (Y1) and polydispersity index (Y2) were selected as the response variables. The experimental design matrix is presented in Table 1. Analysis of variance (ANOVA) was used to evaluate model significance, with $p < 0.05$ considered statistically significant.

Preparation of nanosuspension formulation

The nanoprecipitation method with ultrasonication was used to prepare the nanosuspension. 25 mg of GF was dissolved in 1 mL of acetone to prepare an organic solution, while 10 mL of the aqueous phase was prepared by dissolving different percentages (0.25%, 0.5%, and 0.75%) of previously selected polymer and surfactant in water according to the experimental design in Table 2.

Table 1: Experimental design matrix suggested by Box-Behnken model

Formula	Surfactants (%)	Polymer (%)	Sonication Time (min)
1	0.25	0.5	0
2	0.25	0.75	5
3	0.25	0.25	5
4	0.25	0.5	10
5	0.5	0.75	0
6	0.5	0.5	5
7	0.5	0.75	10
8	0.5	0.25	0
9	0.5	0.25	10
10	0.75	0.75	5
11	0.75	0.5	0
12	0.75	0.25	5
13	0.75	0.5	10
14	0.75	0.75	0
15	0.5	0.5	5
16	0.5	0.5	5
17	0.5	0.5	5

Table 2: Particle size and polydispersity index values of the proposed formulations.

Formula	PS	PDI
N1	2603	0.487
N2	2095	0.29
N3	2987	0.318
N4	2095	0.291
N5	744	0.4
N6	936	0.321
N7	307	0.261
N8	1067	0.3
N9	400	0.262
N10	338	0.245
N11	351	0.359
N12	298	0.202
N13	341.9	0.295
N14	445	0.329
N15	1039	0.329
N16	1096	0.321
N17	882	0.343

Aqueous solutions were filtered through a 0.22 µg syringe. The organic phase was added dropwise (0.5 mL/min) into the precooled aqueous phase maintained in an ice bath under constant magnetic stirring (DRAGONLAB, China) at 1000 rpm to induce precipitation. The nanosuspension was left under stirring at 100 rpm for 2 h to allow the organic solvent to evaporate, then probe sonication (Intelligent Ultrasonic Processor, UCD-150, China) was applied at a power input of 75% of 150 W for varying time durations according to the design (Table 2) using a 5-second on/10-second off cycle. The temperature during sonication was maintained using an ice bath [13].

Measurement of particle size and polydispersity index

By the dynamic light scattering method (DLS) using a Litesizer (Austria), the PS and PDI of the GF nanosuspension formulas were measured. 1 ml of each formula was poured into a polystyrene zeta cell, and measurements were performed at 25°C with a detection angle of 90° [14].

Formula optimization

Numerical optimization was carried out using the desirability function with constraints to PS and PDI, while also defining the desired surfactant level. The optimized formulation predicted by the software was prepared in triplicate to validate the model outputs. The nanosuspension was then centrifuged using a Sigma 3-30K refrigerated centrifuge at 19,000 rpm for 30 min at 4°C, and the supernatant was removed to eliminate excess stabilizers. The resulting pellet was subsequently re-dispersed in deionized water to obtain the optimized nanosuspension formulation [15].

Characterization of the optimized formula

Litesizer (Austria) was used to determine the zeta potential value of the selected GF nanosuspension formula. 1 ml of the NS was loaded into a capillary zeta cell, and the zeta potential was measured [16]. The percentage EE of GF in the formulated NS was anticipated by filtering the supernatant, which was isolated before, through a 0.22 µm filter syringe, and the free drug was calculated and validated, employing the UV-spectrophotometric method [15]. Entrapment percent was calculated using equation 1.

$$\%\ Entrapment\ Efficiency = \frac{Total\ amount\ of\ drug - Free\ Drug}{Amount\ of\ total\ drug\ content} X\ 100\% \quad \ldots\ldots (1)$$

The surface morphology of GF powder and the nanosuspension formulation was examined using field emission-scanning electron microscopy. The coarse drug was imaged using EVO MA10 (Carl Zeiss, UK), while the nanosuspension was examined using Inspect F50 (FEI, Netherlands). In both cases, the samples were mounted on carbon-coated aluminum stubs, dried where applicable, sputter-coated with gold, and imaged under vacuum at different magnifications [17].

Lyophilization of formulas and their recovery

For solid-state conversion, the prepared nanosuspension was subjected to lyophilization using a vacuum freeze dryer (Christ Alpha 1-2 LD plus, Germany). Mannitol or trehalose was used as a cryoprotectant in a 1% ratio to evaluate their ability to provide adequate cryoprotection during lyophilization while minimizing the excipient load and the total solid content of the dried product. NS

samples were frozen overnight at -40°C in a deep freezer, then inserted into the freeze-dryer [18]. The main drying took 24 hours, while the secondary drying took 10 hours. Lyophilized formulations (Lyo-NS) were redispersed in the same volume of DI water to achieve the same concentration of GF before lyophilization and then vortexed for 60 s before being transferred into the cuvettes to measure PS and PDI [19].

Solid-state characterization

Pure GF, a physical mixture that contains GF, PVP, SLS, and cryoprotectant (mannitol or trehalose) in the same ratio used to prepare the formulation, and Lyo-NS formulas were each blended with KBr powder and pressed to form a thin film disc, and then the samples were analyzed using infrared radiation using a Shimadzu 8300 FTIR spectrophotometer (Japan) at a wavenumber of 4000-400 cm [20]. The powder X-ray diffraction (PXRD) of the Lyo-NS and the pure drug was obtained using a diffractometer (Shimadzu XRD-6000, Japan). The instrument was operated at 40 kV and 30 mA in continuous scan mode over a 2θ range of 2–60°, with a step size of 0.05° and a scanning rate of 5°/min [16]. The selected Lyo-NS formula using the optimal cryoprotectant and the pure drug underwent thermodynamic analysis using DSC (Shimadzu, Japan). Weighed 10 mg powder samples were placed in an aluminum-sealed pan and scanned at a heating rate of 5°C/min from 30°C to 250°C in an atmosphere of nitrogen [21].

Drug content

25 mg equivalent of Lyo-NS formulations dissolved in 100 ml of 0.2% water containing SLS. After stirring the mixture with a magnetic stirrer for 30 min. 3 ml of solution was pipetted out and filtered. The concentration of the drug was measured using the UV-spectrophotometric method [22].

The saturated solubility

The phase solubility method was used to determine the solubility of the pure drug and Lyo-NS formulas in water at 25°C and in 0.2% SLS-containing water at 37°C by adding an excess amount of the drug to 10 mL of the above-mentioned media and stirring for 72 hours at 200 RPM in screw-capped tubes. The samples were centrifuged (Hettich, Germany) at 5,000 RPM for 30 min, the supernatant was separated, and the concentration was spectrophotometrically detected [23].

In vitro dissolution study

The *in vitro* dissolution behavior of pure GF and Lyo-NS formulas was performed using USP apparatus II at a rotation speed of 50 rpm and 125 mg of pure GF and its equivalent number of mannitol-based Lyo-NS and trehalose-based Lyo-NS. The dissolution study was performed in 1000 mL of distilled water containing 0.2% SLS, maintained at 37 ± 0.5°C to approximate physiological conditions [8]. At predetermined intervals (5, 15, 30, 45, and 60 minutes), a 5-mL sample was withdrawn, filtered through a 0.22-µm syringe filter, and analyzed by UV–visible spectrophotometry. At each withdrawal, the same volume of medium was compensated with fresh dissolution medium [24].

Stability study

A stability experiment was performed on a trehalose-containing formula at extreme temperature and humidity conditions for 30 days. Using an incubator-desiccator system at 40ºC and 75% relative humidity, where the 75% RH was achieved by saturated sodium chloride in a desiccator [25].

Statistical analysis

Data were statistically analyzed using GraphPad Prism (GraphPad Software 8.3 Inc., CA, USA) at a significant level of 0.05. All data were reported as mean ± SD.

RESULTS

In a preliminary polymer screening step, PVP in combination with SLS produced significantly ($p< 0.05$) the smallest particle size (342 nm); therefore, they were selected as the stabilizers for subsequent studies where sonication was added as a third factor, as designed in Table 2. The combination of formulation factors (polymer and surfactant percent as well as the sonication time) produced nanosuspensions with particle sizes ranging from 298 nm to 2987 nm, as shown in Table 2. The PDI values of all formulations ranged from 0.2 to 0.487, which indicates mid-range polydispersity [26]. Model fitting showed that the quadratic model outperforms others for both PS and PDI, as evidenced by high regression coefficients (R^2), which were 0.989 and 0.963 for PS and PDI, respectively. Experimental data for the particle size (Y1) and PDI (Y2) were analyzed using this model; a high F-value (65 for PS and 17.73 for PDI) and low *p*-value (<0.0006 and 0.0028 for PS and PDI, respectively) further validated the significance of the models. Second-order polynomial regression models were constructed to describe the influence of the independent variables on the response. A positive coefficient in the equations denotes a synergistic influence on the response, whereas a negative coefficient reflects an antagonistic effect. For PS, the equation used was PS = 958.75– 1053.80 A– 155.91 B– 205.23 C+ 238.18 AB+ 119.54 AC+ 52.32 BC+ 622.70 A^2– 95.53 B2–177.30 C^2 … (2)

The ANOVA results (shown in eq. 2 and Figure 1) explain that the surfactant percent (A) was significantly (p= 0.0001) the most inversely influential factor on particle size, followed by sonication time (C) with (p= 0.005) and polymer concentration (B), which has a significantly (p= 0.018) moderate effect. The direction and magnitude of these effects are illustrated in the perturbation plot and Pareto chart (Figure 1A–C), and the response surface plot showed that minimum PS values were obtained at high surfactant levels, moderate polymer concentration, and longer sonication time.

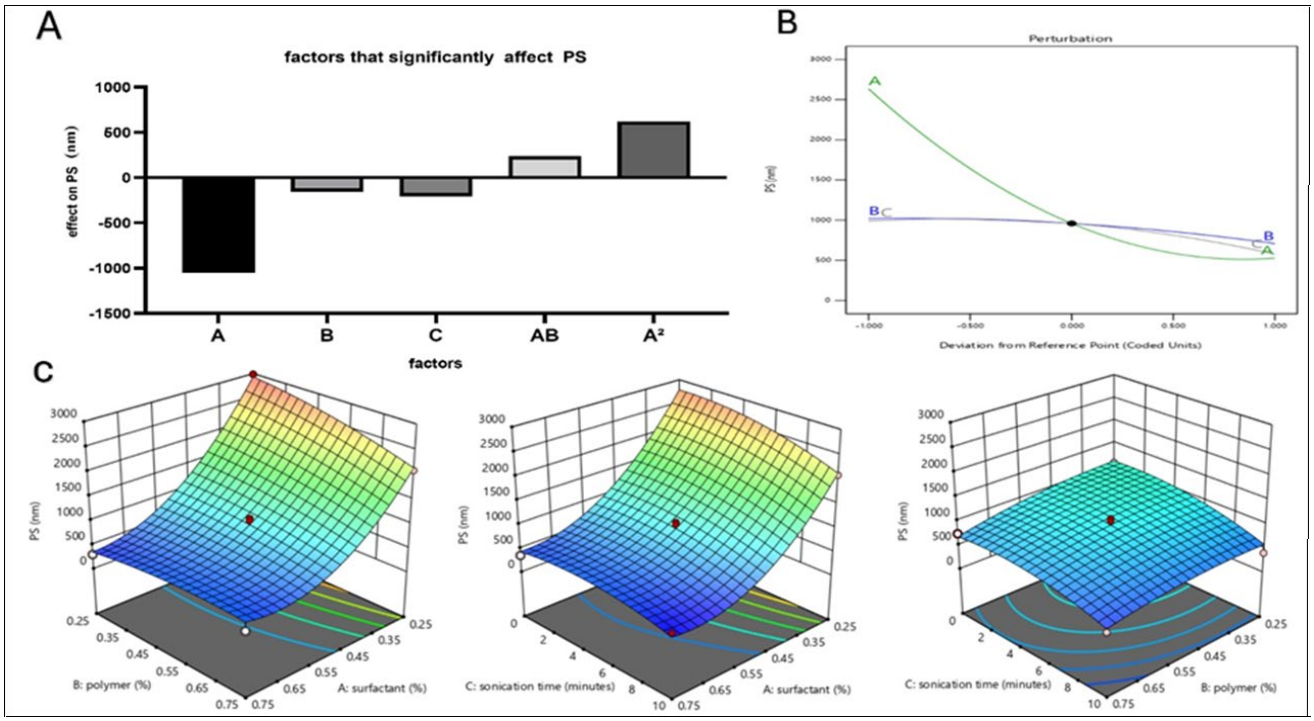

Figure 1: Effect of formulation variables on PS of GF nanosuspension. **A)** Pareto Chart, **B)** Perturbation plot, and **C)** 3D response surface; where **A** is surfactant% , **B** is polymer % and **C** in sonication time.

PDI, which represents size uniformity, is affected by several factors, and a polymodal equation is obtained from the software as PDI = 0.3293– 0.0363 A+ 0.0135 B– 0.0539 C+0.0163 AB+ 0.0344 AC– 0.0238 BC–0.0071A^2– 0.0593 B^2 + 0.0349 C^2 …. (3)

The ANOVA results indicate that sonication time (C) and surfactant% (A) could significantly (p=0.0002 and 0.001, respectively) decrease PDI, while polymer% has no significant (p=0.09) effect, as shown in Figure 2 and equation 3.

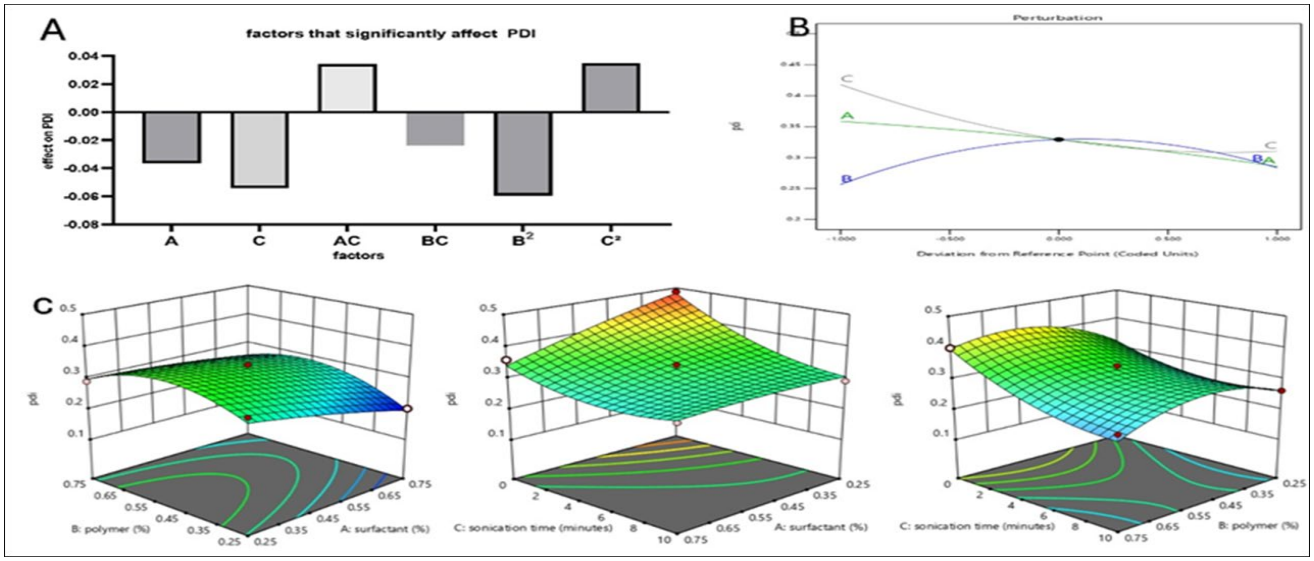

Figure 2: Effect of formulation variables on PDI of GF nanosuspension. **A)** Pareto Chart, **B)** Perturbation plot, and **C)** 3D response surface. Where **A** is surfactant%, **B** is polymer % and **C** in sonication time.

Figure 2C, the 3D response surface, shows that the minimum PDI was obtained at high surfactant, moderate polymer, and extended sonication times, which matches what is needed to obtain minimum PS as mentioned before. The perturbation plot, Figure 2B, shows that factor C (sonication time) has the steepest slope and the strongest influence, followed by surfactant % (A), which aligns with the Pareto chart in Figure 2A. A numerical optimization was carried out using the desirability function with constraints applied. According to the preferred pharmaceutical nanosuspension size range of less than 400 nm [27] and a PDI of 0.1–0.25 for improved physical stability [28], in addition to the preference for the minimum surfactant concentration from the suggested solutions, the optimum formulation was selected with a desirability of 1. To validate the model's predictive accuracy, this predicted optimized formula was then prepared and experimentally evaluated for the target responses. The relative error % of the results was calculated according to equation 4, where the predicted and experimental results were in good agreement, with low percentage relative errors [29], as shown in Table 3.

$$\text{Relative error \%} = \frac{\text{Predicted value} - \text{experimental value}}{\text{predicted value}} \text{ X100\%} \quad (4)$$

The zeta potential of the optimized nanosuspension was −28.7 mV. The entrapment efficiency was 91 ± 4%. The FESEM shows micro-sized defined crystals of the GF, while the NS displays a clear alteration in surface morphology where the particles exhibited a regular shape and a nanometer scale, as demonstrated in Figure 3A-C.

Table 3: The predicted and experimental(observed) values, and corresponding relative errors%, for the optimized formulation

Suggested variables of the optimized formula			Response	Predicted	Observed	Relative Error (%)
A	B	C				
0.6%	0.25%	9.36 min	p.s (nm) PDI	255nm 0.24	264±32.7nm 0.246 ±0.02	3.53% 2.5%

A is surfactant % , B is polymer % and C is sonication time.

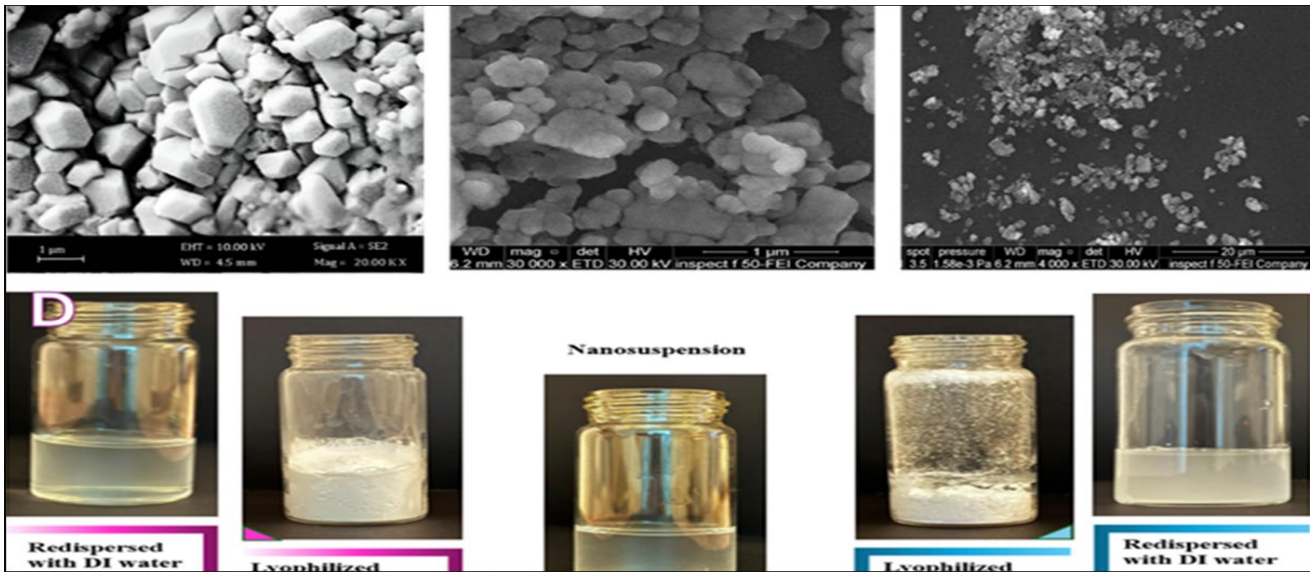

Figure 3: the upper panel shows FE-SEM of **A)** pure Griseofulvin crystals and **(B–C)** optimum NS formula at different magnification power. The lower panel **(D)** shows visual appearance of the fresh nanosuspension, lyophilized cakes prepared with trehalose, and their redispersed forms.

Lyophilization was done using trehalose or mannitol (1% w/v) as cryoprotectants. The trehalose-based formulation showed a well-defined cake with no visible collapse, whereas the mannitol-based formulation showed noticeable shrinkage (Figure 3D). After redispersion, the trehalose-based one showed a particle size of 308 ± 86 nm, while the mannitol-based nanosuspension showed a mean particle size of 843 ± 23 nm. The FTIR spectra of pure GF, Lyo-NS formulations, and physical mixtures (containing GF, PVP, SLS, and cryoprotectant (mannitol or trehalose) in the same ratio used to prepare the formulations) are presented in Figure 4. The characteristic GF peaks observed at 3294, 2943, 2837, 2559.71, 1502, 1656, 1705, and 1776 cm^{-1} correspond to various stretching vibrations of single bonds (CH stretch) and double bonds (C=O, C=C, C=N) present in GF [30]. The spectra of the physical mixtures and lyophilized formulations showed the main characteristic peaks of GF with reduced intensity, slight broadening, and minor peak shifts within the same functional group regions. These changes are summarized in Table 4. Powder X-ray diffraction was carried out for the GF powder and for the Lyo-NS. As shown in Figure 5A, the pure drug exhibits intense and sharp diffraction peaks (Bragg peaks) at 10.6°, 13.8°, 14.4°, 16.4°, 23.7°, 26.5°, and 28.4°. In contrast, the mannitol-based Lyo-NS formulation showed a marked reduction in both the number and intensity of the diffraction peaks.

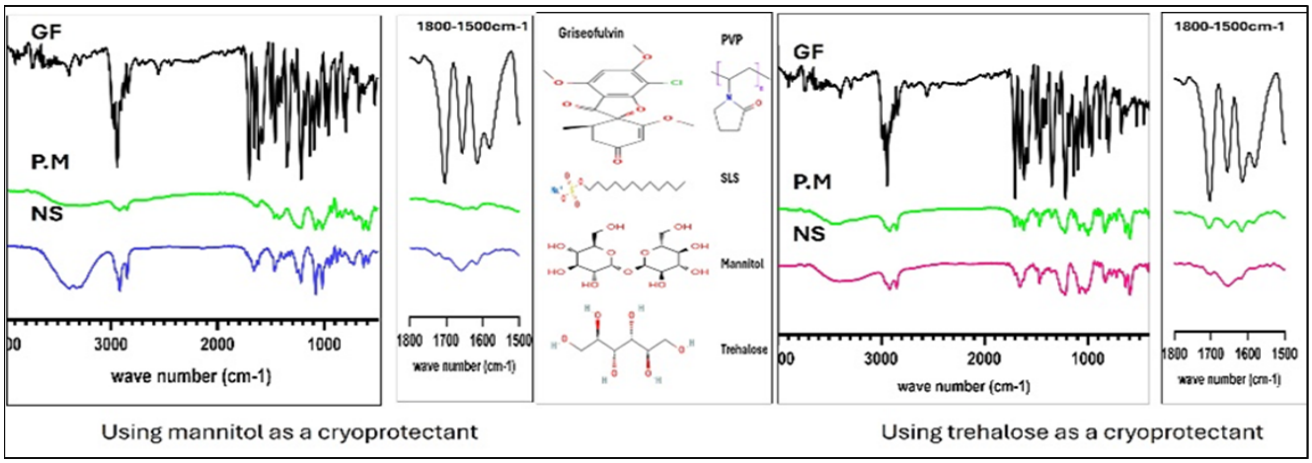

Figure 4: FTIR spectrum of the GF and physical mixture (containing GF,SLS,PVP and mannitol or trehalose in the same ratios in the formulation) and the lyophilized nanosuspension.

Table 4: FTIR peaks of pure Griseofulvin, physical mixture (P.M), and GF nanoparticle

Functional group	Pure GF	Using mannitol as cryoprotectant		Using trehalose as cryoprotectant	
		P.M	Nanocrystals	P.M	Nanocrystals
C=O stretch; benzofuranone ring carbonyl	1705 Sharp and strong	1705 Shoulder band	1705 shoulder band;1730 weak and broader	1707 sharp and strong	1701 shoulder band
C=O stretch; cyclohexanone carbonyl	1656 Sharp, medium	1653 Broad, medium	1656 Broad, medium	1656 sharp and medium	1653 broad band
C=C stretch; aromatic and cyclic unsaturation	1616 Sharp, medium	1618 sharp and medium	1616 Sharp, Medium	1658 Sharp and medium	1620 shoulder band

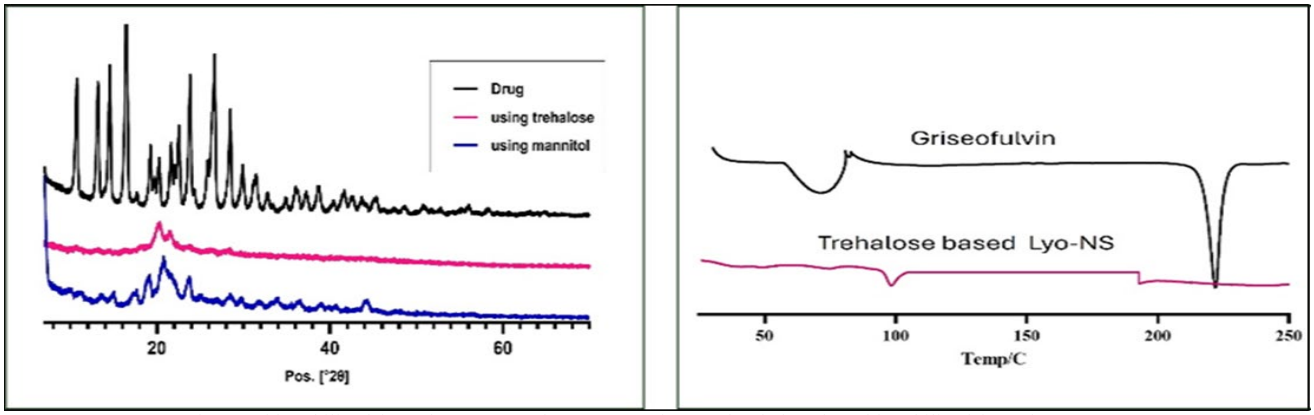

Figure 5: **A)** XRPD of GF and lyophilized formulas. **B**) DSC thermogram of GF and trehalose-based lyophilized formula.

This effect was even more pronounced in the trehalose-based formulations, which exhibited a halo pattern. Therefore, DSC analysis was performed for the trehalose-based Lyo-NS to further confirm the amorphization. DSC thermograms are shown in Figure 5B. Pure GF exhibited an endothermic peak at 221°C and a broad event at 50–100°C. The Lyo-NS thermograms showed the disappearance of the 221°C peak and the presence of peaks at 192°C and 97°C in the trehalose-based Lyo-NS. The drug content of the mannitol-based formulation was 87.5 ± 1.4%, while that of the trehalose-based formulation was 89.12 ± 2.3%. The saturated solubility of pure griseofulvin in water was ≈0.05 mg/L, which is consistent with the published data [31]. In both media, lyo-NS had significantly (p< 0.05) higher solubility values compared to pure GF. Between the two lyophilized formulations, the trehalose-based NS showed markedly higher solubility than the mannitol- based NS in both test media. In water, the trehalose formulation achieved a solubility of 0.37 mg/mL compared with 0.14 mg/mL for the mannitol. formulation. Similarly, in 0.2% SLS solution, the trehalose-based NS reached 0.87 mg/mL, whereas the mannitol-based NS showed a solubility of 0.46 mg/mL. These differences were statistically significant (p= 0.001). The *in vitro* dissolution study, Figure 6, revealed that both the lyophilized nanosuspension formulations exhibit better release profiles than the pure drug, with a 96.3% release rate for the trehalose-containing formula and 72.5% for the mannitol-containing formula compared with only

37.8% for the pure drug in the first 15 min. The trehalose-based lyophilized nanosuspension stored for 30 days under accelerated temperature and humidity conditions showed a PS of 359 ± 41 nm, a PDI of 0.36 ± 0.07, and a drug content of 89.1 ± 0.9%.

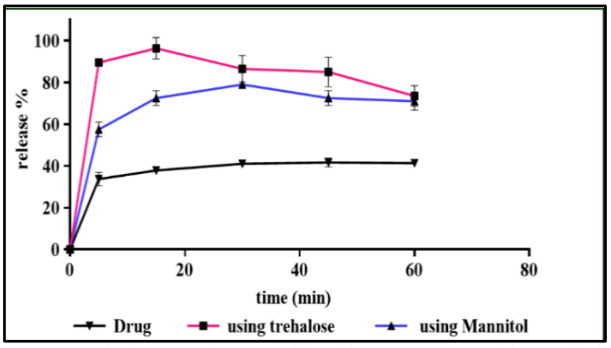

Figure 6: The in *vitro* release profile of the GF, Lyo-NS with mannitol, and Lyo-NS with trehalose.

DISCUSSION

The BBD results and quadratic models confirmed that surfactant percentage in the formulation was the most critical factor controlling PS, followed by sonication time, then polymer concentration. This could be explained by SLS having an anionic nature that imparts a negative surface charge to the particles, thereby causing electrical repulsion that prevents the agglomeration. In addition, SLS acts as a wetting agent that reduces the surface tension [32]. On the other hand, PVP is a non-ionic polymer that prevents particle growth and agglomeration by adsorbing on the crystal surfaces, therefore forming a hydrodynamic boundary layer around the particles (steric stabilization) [33]. The presence of polymer-coated particles also reduces Brownian motion, limiting particle–particle collisions and inhibiting the attachment and detachment of molecules on particle surfaces, thereby suppressing aggregation. [34]. Ultrasonication significantly reduces particle size by breaking down agglomerates through cavitation-induced mechanical forces such as shockwaves and microstreaming [35]. Consistent with previous studies, our findings showed a clear downward trend in particle size with increased sonication time. This indicates that applying sufficient ultrasonication time is effective for decreasing particle size, provided that the suspension temperature remains low during sonication by using an ice bath to prevent reaggregation [36]. According to Sharma *et al*., the use of PVP and SLS resulted in superior PS reduction in the presence of ultrasonic energy [37]. For PDI, increasing sonication time leads to a substantial reduction in PDI due to enhanced dispersion and particle breakage. One study reported the coexistence of distinct crystal morphologies (including larger octahedral particles and smaller flake-like structures) when griseofulvin precipitated in the presence of PVP without the application of sonication [38]. The influence of sonication was also demonstrated in a study on azithromycin nanosizing, where ultrasound-assisted precipitation conducted at temperatures below 10°C resulted in a narrower size distribution [39]. SLS concentration showed a lesser effect on PDI, where it stabilizes the particles, thus ensuring uniform distribution. The predictability and reliability of the design were tested, and the low relative error indicates the adequacy and reliability of the developed quadratic model [29]. These findings are consistent with the recent studies that highlight the growing importance of combining formulation technology with systematic optimization tools such as Quality by Design to enhance formulation robustness and practical applicability [40]. The zeta potential (−28.7 mV) suggests that electrostatic repulsion due to SLS combined with adsorbed PVP chains forms an electrosteric barrier. It is considered sufficient to prevent aggregation in nanosuspensions, as zeta potentials of ±20 mV or higher are generally acceptable for electrosteric systems [41]. The high entrapment efficiency (91 ± 4%) may be slightly reduced by drug binding to excess surfactant or solubilizing in the supernatant, as reported in other surfactant-rich nanosuspension systems [42]. Trehalose provided superior cryoprotection during lyophilization compared with mannitol, as indicated by lower post-drying particle size and improved cake morphology. This observation aligns with literature reports describing trehalose as a glass-forming excipient capable of preserving nanoparticles during freezing and drying. On the other hand, mannitol tends to crystallize and offers less effective protection against the aggregation [43]. PXRD findings show characteristic Bragg peaks of GF, indicating its crystallinity, which aligns with previous studies [44]. A reduction in crystallinity in the mannitol-based formulation was suggested due to particle-size reduction and disruption of the crystal lattice during nanoprecipitation, as well as the process stress. This effect was more pronounced in the trehalose-based formulation, which showed a marked loss of crystalline and a predominantly amorphous character [45]. This was confirmed by the DSC thermogram, where the GF sharp melting peak at 221°C confirms the crystallinity of the drug [8]. This peak disappeared in trehalose-based Lyo-NS, which suggests amorphization. A small peak at 192°C has appeared, which could be the SLS peak or overlapping thermal events of SLS and anhydrous trehalose that formed during the drying [46]. These observations are consistent with previous findings reported by Alshweiat *et al*., who demonstrated that the reduction in drug crystallinity in loratadine nanosuspensions could be attributed to interactions between the drug and the surfactant or cryoprotectant, in addition to the mechanical and thermal stresses imposed during the drying process, which collectively contribute to partial or complete drug amorphization [47]. Reduced crystallinity and smaller particle size contributed to the significantly enhanced solubility and dissolution

behavior observed compared with pure griseofulvin. This is consistent with previous findings reported by Kral *et al*., who developed lidocaine nanosuspension using a wet media milling approach utilizing Design Expert to optimize the formulation parameters [48]. The authors demonstrated that particle size reduction to the nanometer range significantly improved the dissolution behavior of lidocaine. The trehalose-based nanosuspension also demonstrated superior solubility compared with the mannitol-based formulation, which correlates with higher amorphous content. In addition, a smaller PS, as described by the Ostwald–Freundlich relation, leads to increased saturation solubility because the surface free energy rises as the particle radius decreases [49]. The enhanced drug dissolution behaviors of the freeze-dried NS relative to the pure drug are attributed to combined factors including the loss of drug crystallinity during drying, particle size reduction with its associated increase in surface area, and the presence of surfactant coating, resulting in instantaneous dissolution [50]. Lyo-NS containing trehalose outperforms the mannitol-based formulation in *vitro* dissolution performance, which is consistent with the above obtained data (higher saturated solubility and smaller particle size). This is because dissolution is directly proportional to saturated solubility and inversely proportional to particle size according to the Noyes-Whitney equation [18,6]. Trehalose was chosen as the optimum cryoprotectant based on the aforementioned results. Furthermore, the trehalose-based nanosuspension maintained nanoscale particle size and acceptable drug content following accelerated storage, indicating satisfactory short-term physical stability. This effect is due to the ability of trehalose to immobilize particles and reduce the risk of aggregation [50]. These observations underscore the value of nanosuspensions as an effective, innovative formulation strategy for rigid, hydrophobic BCS Class II drugs such as griseofulvin, and address the challenges of converting the nanosuspension to solid form as reported in recent studies [4].

Study limitations

This work is needed to evaluate different trehalose levels to determine the optimal concentration for preserving particle size distribution and structural integrity after freeze-drying. In addition, it should be noted that the stability data presented in this study reflect short-term stability only, and long-term stability studies are required to fully assess the physical stability of the formulation.

Conclusion

In this study, a stable and optimized griseofulvin nanosuspension was successfully developed using an ultrasonication-assisted antisolvent precipitation technique utilizing Box–Behnken experimental design. Systematic stabilizer screening showed that combining PVP K30 and SLS provided superior particle size reduction through synergistic steric and electrostatic mechanisms. BBD analysis confirmed that surfactant % and sonication time were the most influential factors associated with low particle size and size distribution. The optimized formulation achieved 264 nm and PDI 0.249, entrapment efficiency of 91%, and excellent colloidal stability. Lyophilization with trehalose effectively preserved nanoparticle characteristics with good redispersibility. Solid-state analyses demonstrated a marked reduction in crystallinity and partial amorphization of griseofulvin, which directly translated into significantly enhanced saturated solubility and a rapid dissolution profile.

ACKNOWLEDGMENT

The authors thank the Mustansiriyah University, College of Pharmacy, for supporting the project.

Conflict of interests

The authors declared no conflict of interest.

Funding source

The authors did not receive any source of funds.

Data sharing statement

Supplementary data can be shared with the corresponding author upon reasonable request.

REFERENCES

1. Dhudum R, Ganeshpurkar A, Pawar A. Revolutionizing drug discovery: A comprehensive review of AI applications. *Drugs Drug Candidates*. 2024;3(1):148-171. doi: 10.3390/ddc3010009.
2. Truzzi F, Tibaldi C, Zhang Y, Dinelli G, D′ Amen E. An overview on dietary polyphenols and their biopharmaceutical classification system (BCS). *Int J Mol Sci*. 2021;22(11):5514. doi: 10.3390/ijms22115514.
3. Bhalani DV, Nutan B, Kumar A, Singh Chandel AK. Bioavailability enhancement techniques for poorly aqueous soluble drugs and therapeutics. *Biomedicines*. 2022;10(9):2055. doi: 10.3390/biomedicines10092055.
4. Jacob S, Kather FS, Boddu SHS, Attimarad M, Nair AB. Nanosuspension innovations: Expanding horizons in drug delivery techniques. *Pharmaceutics*. 2025;17(1):136. doi: 10.3390/pharmaceutics17010136.
5. Chavhan R. Nanosuspensions: Enhancing drug bioavailability through nanonization. *Ann Pharm Fr*. 2025;83(2):251-271. doi: 10.1016/j.pharma.2024.06.003.
6. Noyes AA, Whitney WR. The rate of solution of solid substances in their own solutions. *J Am Chem Soc*. 1897;19:930-934. doi: 10.1021/ja02086a003.
7. Nguyen HX, Le NY, Nguyen CN. Quality by design optimization of formulation variables and process parameters for enhanced transdermal delivery of nanosuspension. *Drug Del Transl Res*. 2025;15(6):2220-2251. doi: 10.1007/s13346-024-01733-4.
8. USP. Griseofulvin United States Pharmacopeia 43 – National Formulary 38. Rockville, MD: United States Pharmacopeial Convention; 2020. p. 3008-11.

9. Aris P, Wei Y, Mohamadzadeh M, Xia X. Griseofulvin: An updated overview of old and current knowledge. *Molecules*. 2022;27(20):7034. doi: 10.3390/molecules27207034.
10. Kumar R, Siril PF. Controlling the size and morphology of griseofulvin nanoparticles using polymeric stabilizers by evaporation-assisted solvent–antisolvent interaction method. *J Nanopart Res*. 2015;17(6):256. doi: 10.1007/s11051-015-3066-6.
11. Li M, Alvarez P, Orbe P, Bilgili E. Multi-faceted characterization of wet-milled griseofulvin nanosuspensions for elucidation of aggregation state and stabilization mechanisms. *AAPS PharmSciTech*. 2018;19(4):1789-801. doi: 10.1208/s12249-018-0993-4.
12. Sigfridsson K, Rydberg H, Strimfors M. Nano- and microcrystals of griseofulvin subcutaneously administered to rats resulted in improved bioavailability and sustained release. *Drug Dev Ind Pharm*. 2019;45(9):1477-1486. doi: 10.1080/03639045.2019.1628769.
13. Elshafeey AH, El-Dahmy RM. Formulation and development of oral fast-dissolving films loaded with nanosuspension to augment paroxetine bioavailability: In vitro characterization, ex vivo permeation, and pharmacokinetic evaluation in healthy human volunteers. *Pharmaceutics*. 2021;13(11):1869. doi: 10.3390/pharmaceutics13111869.
14. Abbas AF, Ashoor JA, Alamir HTA. Preparation and characterization of fluocinolone acetonide as nanosuspension based hydrogel for topical skin administration. *Al Mustansiriyah J Pharm Sci*. 2026;25(5):682-696. doi: 10.32947/ajps.v25i5.1201.
15. Ghose D, Patra CN, Ravi Kumar BVV, Swain S, Jena BR, Choudhury P, et al. QbD-based formulation optimization and characterization of polymeric nanoparticles of cinacalcet hydrochloride with improved biopharmaceutical attributes. *Turk J Pharm Sci*. 2021;18(4):452-464. doi: 10.4274/tjps.galenos.2020.08522.
16. Abd-Alhammid SN, Kadhum RW. Process factors affecting the preparation and characterization of dutasteride nanosuspension. *Iraqi J Pharm Sci*. 2025;34(1):35-48. DOI: doi: 10.31351/vol34iss1pp35-48.
17. Mohammed-Kadhum MF, Hameed GS. Development and characterization of furosemide-loaded binary amorphous solid dispersion to enhance solubility and dissolution for pediatric oral administration. *Pharmacia*. 2025;72:1-19. doi: 10.3897/pharmacia.72.e156784.
18. Mohammed AA, Abd Alhammid SN. Preparation, in vitro evaluation and characterization studies of clozapine nanosuspension. *Iraqi J Pharm Sci*. 2024;33(4SI)):336-348. doi: 10.31351/vol33iss(4SI)pp336-348.
19. Gülbağ Pınar S, Pezik E, Mutlu Ağardan B, Çelebi N. Development of cyclosporine A nanosuspension: cytotoxicity and permeability on Caco-2 cell lines. *Pharm Dev Technol*. 2022;27(1):52-62. doi: 10.1080/10837450.2021.2020817.
20. Alwan RM, Rajab NA. Nanosuspensions of selexipag: formulation, characterization, and in vitro evaluation. *Iraqi J Pharm Sci*. 2021;30(1):144-153. doi: 10.31351/vol30iss1pp144-153.
21. Hussein AM, Hameed G, Aziz FM. Improve the solubility of cefpodoxime proxetil by amorphous solid dispersion technique. *J Res Pharm*. 2025;29(4):1437-1450. doi: 10.12991/jrespharm.1734450.
22. Thorat S, Singh M, Tare M. Bioavailability enhancement of abiraterone acetate through quercetin-loaded nanoparticles. *Palest Med Pharm J*. 2025;11(3). doi: 10.59049/2790-0231.11.3.2502.
23. Maded ZK, Sfar S, Taqa GAA, Lassoued MA, Ben Hadj Ayed O, et al. Development and optimization of dipyridamole- and roflumilast-loaded nanoemulsion and nanoemulgel for enhanced skin permeation: Formulation, characterization, and in vitro assessment. *Pharmaceuticals*. 2024;17(6). doi: 10.3390/ph17060803.
24. Porwal O. Box-Behnken design-based formulation optimization and characterization of spray dried rutin loaded nanosuspension: State of the art. *South Afr J Bot*. 2022;149:807-815. doi: 10.1016/j.sajb.2022.04.028.
25. Naama NA, Hameed GS, Hanna DB, Mahdi ZH. Formulation of cefdinir ternary solid dispersion and stability study under harsh conditions. *Al Mustansiriyah J Pharm Sci*. 2025;25(1):27-48. doi: 10.32947/ajps.v25i1.1106.
26. Alhagiesa AW, Ghareeb MM. The Formulation and characterization of nimodipine nanoparticles for the enhancement of solubility and dissolution rate. *Iraqi J Pharm Sci*. 2021;30(2):143-152. doi: 10.31351/vol30iss2pp143-152.
27. Leung DH. Development of nanosuspension formulations compatible with inkjet printing for the convenient and precise dispensing of poorly soluble drugs. *Pharmaceutics*. 2022;14(2). doi: 10.3390/pharmaceutics14020449.
28. Qureshia MJ, Phina FF, Patrob S. Enhanced solubility and dissolution rate of clopidogrel by nanosuspension: formulation via high pressure homogenization technique and optimization using Box Behnken design response surface methodology. *J Appl Pharm Sci*. 2017;7(2):106-113. doi: 10.7324/JAPS.2017.70213.
29. Patel J, Dhingani A, Garala K, Raval M, Sheth N. Quality by design approach for oral bioavailability enhancement of Irbesartan by self-nanoemulsifying tablets. *Drug Deliv*. 2014;21(6):412-435. doi: 10.3109/10717544.2013.853709.
30. Sreeharsha N, Prasanthi S, Rao GSNK, Gajula LR, Biradar N, Goudanavar P, et al. Formulation optimization of chitosan surface coated solid lipid nanoparticles of griseofulvin: A Box-Behnken design and in vivo pharmacokinetic study. *Eur J Pharm Sci*. 2025;204:106951. doi: 10.1016/j.ejps.2024.106951.
31. Galipeau K, Socki M, Socia A, Harmon PA. Incomplete loading of sodium lauryl sulfate and fasted state simulated intestinal fluid micelles within the diffusion layers of dispersed drug particles during dissolution. *J Pharm Sci*. 2018;107(1):156-169. doi: 10.1016/j.xphs.2017.06.006.
32. Che Mohamed Hussein SN, Amir Z, Jan BM, Khalil M, Azizi A. Colloidal stability of CA, SDS and PVA coated iron oxide nanoparticles (IONPs): Effect of molar ratio and salinity. *Polymers*. 2022;14(21):4787. doi: 10.3390/polym14214787.
33. Karakucuk A, Celebi N. Investigation of formulation and process parameters of wet media milling to develop etodolac nanosuspensions. *Pharm Res*. 2020;37(6):111. doi: 10.1007/s11095-020-02815-x.
34. Zhang Y, Li B, Liu J, Han D, Rohani S, Gao Z, et al. Inhibition of crystal nucleation and growth: A review. *Cryst Growth Des*. 2024;24(6):2645-2665. doi: 10.1021/acs.cgd.3c01345.
35. Siddique M, Rashid R, Ali A. Fundamentals of acoustic cavitation, ultrasound-assisted processes, and sonochemistry. Modeling and Simulation of Sono-Processes: Elsevier; 2025. p. 3-17.
36. Gokce Y, Cengiz B, Yildiz N, Calimli A, Aktas Z. Ultrasonication of chitosan nanoparticle suspension: Influence on particle size. *Colloids and Surfaces A*. 2014;462:75-81. doi: 10.1016/j.colsurfa.2014.08.028.
37. Sharma C, Desai MA, Patel SR. Effect of surfactants and polymers on morphology and particle size of telmisartan in ultrasound-assisted anti-solvent crystallization. *Chem Papers*. 2019;73(7):1685-1694. doi: 10.1007/s11696-019-00720-1.
38. Prasad R, Dalvi SV. Understanding morphological evolution of griseofulvin particles into hierarchical microstructures during liquid antisolvent precipitation. *Cryst Growth Des*. 2019;19(10):5836-5849. doi: 10.1021/ACS.CGD.9B00859.
39. Sabnis SS, Singh SD, Gogate PR. Improvements in azithromycin recrystallization using ultrasound for size reduction. *Ultrason Sonochem*. 2022;83:105922. doi: 10.1016/j.ultsonch.2022.105922.
40. Khan A, Naquvi KJ, Haider MF, Khan MA. Quality by design-newer technique for pharmaceutical product development. Intelligent Pharmacy. 2024;2(1):122-9.
41. Kaplan ABU, Öztürk N, Çetin M, Vural I, Özer TÖ. The nanosuspension formulations of daidzein: Preparation and in vitro characterization. *Turk J Pharm Sci*. 2022;19(1):84. doi: 10.4274/tjps.galenos.2021.81905.
42. Patel GV, Patel VB, Pathak A, Rajput SJ. Nanosuspension of efavirenz for improved oral bioavailability: formulation optimization, in vitro, in situ and in vivo evaluation. *Drug Dev Ind Pharm*. 2014;40(1):80-91. doi: 10.3109/03639045.2012.746362.
43. Pandita D, Ahuja A, Velpandian T, Lather V, Dutta T, Khar R. Characterization and in vitro assessment of paclitaxel loaded lipid nanoparticles formulated using modified solvent injection technique. *Pharmazie*. 2009;64:301-10. PMID: 19530440.

44. Almalik A, Alradwan I, Kalam MA, Alshamsan A. Effect of cryoprotection on particle size stability and preservation of chitosan nanoparticles with and without hyaluronate or alginate coating. *Saudi Pharm J*. 2017;25(6):861-867. doi: 10.1016/j.jsps.2016.12.008.
45. Townley ER. Griseofulvin. In: Florey K, editor. Analytical Profiles of Drug Substances. Vol.8. Academic Press; 1979. p. 219-49.
46. Zahraa AA, Fatima JJ. Preparation and Evaluation of Lercanidipine HCl Nanosuspension to Improve the Dissolution Rate. *Iraqi J Pharm Sci*. 2025;33((4SI)):20-30. doi: 10.31351/vol33iss(4SI)pp20-30.
47. Kral O, Ilbasmis-Tamer S, Han S, Tirnaksiz F. Development of dermal lidocaine nanosuspension formulation by the wet milling method using experimental design: in vitro/in vivo evaluation. *ACS omega*. 2024;9(52):50992-1008.
48. Alshweiat A, Katona G, Csóka I, Ambrus R. Design and characterization of loratadine nanosuspension prepared by ultrasonic-assisted precipitation. *Eur J Pharm Sci*. 2018;122:94-104. doi: 10.1016/j.ejps.2018.06.010.
49. Rashed M, Dadashzadeh S, Bolourchian N. The impact of process and formulation parameters on the fabrication of Efavirenz nanosuspension to improve drug solubility and dissolution. *Iran J Pharm Res*. 2022;21(1):e129409. doi: 10.5812/ijpr-129409.
50. Ambrus R, Alshweiat A, Szabó-Révész P, Bartos C, Csóka I. Smartcrystals for efficient dissolution of poorly water-soluble meloxicam. *Pharmaceutics*. 2022;14(2):245. doi: 10.3390/pharmaceutics14020245.